Research Article | Vol. 11, No. 7 / 1 July 2021 / Optical Materials Express 2288
Optical Materials EXPRESS

Few-mode elastomeric optical fibers

MIGUEL LLERA,* FRÉDÉRIC FLAHAUT, SYLVAIN BERGERAT, JUSTIN BENOIT, ROWAN LÜTHI, FRÉDÉRIC MATHEZ, SÉBASTIEN LE FLOCH, AND YVES SALVADÉ

Haute Ecole Arc Ingénierie, Haute Ecole Spécialisée de Suisse Occidentale, Rue de la Serre 7, 2610 Saint-Imier, Switzerland
Miguel.llera@he-arc.ch

Abstract: We present a new approach for producing elastomeric optical fibers with an optical behaviour corresponding to a few-mode optical fiber. Different fibers have been produced by first fabricating thermoplastic polyurethane preforms and subsequently drawing them. The fiber attenuation has been measured by the cut-back technique and the fiber bending transmission tolerance evaluated. The fiber potential has been assessed through two basic experiments in order to highlight the benefits of elasticity and a reduced core diameter. Future potential of the proposed fiber is discussed and shows a very auspicious path towards new and unexplored applications.

1. Introduction

Optical fibers are today a very well-known technology that was mainly driven by communications applications at its early days [1]. Since then, many things have changed and new fiber designs and materials have emerged that have allowed new light manipulations and applications. The medical field is an area with a huge interest in research for optical fibers. Applications can be found for imaging, spectroscopy, endoscopy, tissue pathology, blood flow monitoring, light therapy, biosensing, biostimulation, laser surgery, dentistry, dermatology, and health status monitoring [2]. Nevertheless, many of these applications are temporal processes that are performed during a surgery or during a specific medical treatment. Creating permanent implants that use optical fibers face the problem of the biocompatibility of the standard materials used to fabricate the fibers [3,4]. Additionally, some applications could potentially use tiny optical fibers to bring light in sensitive areas where an optical fiber breakage could damage organs [5].

Traditional glass optical fibers can be found today in many types and configurations but they present an important safety issue related to their rigidity and a high hazardous breakability together with biocompatibility issues for long-term applications. Some efforts are done in order to find solutions to avoid the use of such fibers [6] but biocompatible and safe optical fibers would ease some treatments or specific sensing. Plastic optical fibers could be better candidates but they still suffer from plastic deformations and are to be avoided in applications where complex or extreme manipulations are needed. In some cases, organ-scale lengths are enough but other applications need longer fibers lengths making it very important to be able to produce highly flexible fibers on much longer scales. Therefore, using optical fibers made from elastomeric materials that can be found on a medical grade could have a significant impact for medical applications. Elastomeric materials have also a Young's modulus that is much closer to those observed in natural tissues [7] making them more adapted for designing safer optical fibers.

Because of these material and mechanical constraints, soft and polymeric biomaterials, for producing fibers with reduced stiffness, have been proposed in the last years. Among all the different varieties we may highlight the work done on silk fibroin [8] and hydrogels [9–11]. Silk fibroin can be interesting for temporal applications where the fiber is needed to be resorbed into the body after its use. But this biodegradability can be a drawback for long-term applications as

#428585 https://doi.org/10.1364/OME.428585
Journal © 2021 Received 21 Apr 2021; revised 18 Jun 2021; accepted 19 Jun 2021; published 23 Jun 2021

Optical Materials EXPRESS

for implants. Another weakness is that the fiber makes use of the surrounding air to achieve the total internal reflection, which can obviously be an issue when the fiber is implanted. Hydrogel fibers are better candidates as they can be degradable or not and a cladding can be added onto the core by dipping it in a sodium alginate and calcium chloride solution for a few minutes. Nevertheless, the fibers produced have great core diameters (> 340 µm) and are highly multimode. The core/cladding refractive index contrast flexibility is also difficult to realize. However, there are also other materials that can potentially be used to produce optical fibers for medical applications like silicones [12] or polyurethanes (PU) [13]. These last two material families are also biocompatible as medical grade silicones can be used for medical tubing, implants [14] and PU has applications in medical fields [15]. Silicone fibers have been studied for a long time and a patent for those fibers has already been submitted in 1991 [16]. The fabrication of such fiber is done by dipping an extruded core into a cladding solution and then by curing the cladding. However, this is extremely complex and impracticable to produce such fibers when core diameters down to a few µm are needed to ensure a single-mode, or a few modes behaviour. PU fibers as described in [13] make use of commercially available PU tubes to produce a hollow waveguide preform by the stack-and-draw procedure. They are then limited to what is available in the market concerning shapes and sizes. The guiding mechanism relies on a grazing incidence guidance making the fiber very sensitive to bend losses and the transmission losses are important (0.54 dB/cm) despite the light propagates in air. Another configuration proposed in [17] makes also use of commercially available PU tubes to produce antiresonant fibers. However, this work was at THz wavelengths and scaling to the visible would seem impractical due to the very thin core boundaries (0.3 µm) [18] needed.

Another important aspect regarding a possible highly stretchable optical fiber is its guiding behaviour. Most of the proposed solutions generate highly multimode fibers (MMF). They could be very interesting for some applications as lightning or low bandwidth transmissions. But for high bandwidth transmissions or for interrogating sensors as Fabry-Pérot fiber tips, a few modes or single-mode behaviour would be needed. As an example, in a Fabry-Pérot resonating cavity, interferences are observed due to the superposition of phase delayed coherent light waves. In such cavity located at the tip of a single-mode optical fiber, resonance gives an interferometric fringe pattern whose characteristics will depend on the cavity length and mirrors quality. However, when using MMF we may have several temporal modes resonating in the cavity and each of them having their own initial phase due to the well-known modal dispersion in the fiber. This will have a direct consequence on the interferometric fringe pattern quality and its visibility is decreased [19]. It is demonstrated that the fringe visibility is decreased by increasing the number of modes for a determined resonating cavity length. Therefore, in order to increase the fringe visibility, excited modes number must be reduced or the modal dispersion would need to be decreased. This last can be reduced much easily on polymer optical fibers due to the strong mode coupling coefficient induced by material impurities and waveguide imperfections [20].

In this paper, we propose a new approach to produce biocompatible and highly stretchable step-index optical fibers by using low-cost, biocompatible and optically transparent thermoplastic polyurethane (TPU) with a much more reduced multimode behaviour. The general idea remains in the production, by injection molding, of an initial TPU preform that can be configured to match a specific fiber configuration need. The preform is then drawn by a classical drawing process. The manuscript is organized such a way that the fabrication process is first described and followed by the principle fiber characteristics of several produced fibers. Then, some potential applications are evaluated through exploratory tests and finally a discussion is brought in order to highlight the potential of the proposed fiber.

Optical Materials EXPRESS

2. TPU optical fibers: processes and characteristics

2.1. Fabrication procedure and produced fibers

TPU is a well-known thermoplastic elastomer whose elastomeric properties are the result of a segmented block copolymer consisting of alternating flexible and rigid segments [21]. The rigid segments consist essentially of glassy and/or semi-crystalline butanediol and diisocyanate units and the flexible segments of long-chain polyether or polyester polyols. It is that alternating arrangement between those flexible and rigid segments, as shown in Fig. 1, that gives the elastomeric property to the material. When processing such material, we face two different glass transition temperatures: One for the flexible segment, T_{g1}, and another one to the rigid segment, T_{g2}, where $T_{g2} > T_{g1}$. Basically, the material will need to be used between those two temperatures as for temperatures $T < T_{g1}$, both segments are hard and brittle and for $T > T_{g2}$, the material will start to be a viscous fluid. That is of importance for the production of an optical fiber due to the fact that weakly guiding fibers need a step refractive index and hence two different TPUs in our case. Care need to be taken in the choice of the two TPUs needed to produce the step-index profile. T_{g1} temperatures are usually well below the 0°C temperature and are of less concern in the choice. However, T_{g2} will have a direct influence in the fiber drawing as one of the two TPUs could start to melt at a lower temperature than the second one. Furthermore, the heating system, if not correctly designed, will generate a radially graded heat distribution into the preform possibly increasing the glass transition temperature difference effect. The two TPUs we have chosen to produce an optical fiber are BASF Elastollan 1185A and Elastollan 1185 A10W having refractive indexes, $n_{d,}$ of 1.505 and 1.553, respectively. The processing temperatures for both TPUs are given to be relatively similar. However, the glass transition temperatures, listed in Table 1, are different and consequently, we had to increase the heating temperature of at least 10°K above the processing temperature of 1185A alone to get a smoother fiber drawing.

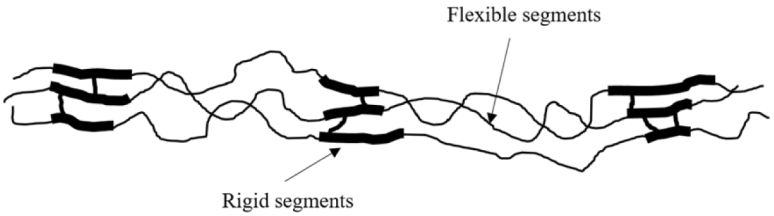

Fig. 1. Structure of the alternated rigid and flexible segments of a typical TPU.

Table 1. Glass transition and melting temperatures for BASF TPU (courtesy of BASF)

TPU	T_{g1} [°C]	T_{g2} [°C]	Melting temperature [°C]
1185A	−63	67	221
1185 A10W	−35	92	248

The fiber preform is realized in a two-step injection molding process using an Arburg Allrounder 170S injection machine. First injection is performed in a cylindrical cavity having dimensions of 15 mm in diameter for 100 mm in length with a cylindrical insert in the middle along the cavity axis. The role of the insert is to produce a preform with a central hole. This first step preform generates the cladding part of the fiber by using the Elastollan 1185A TPU. A second injection, using the Elastollan 1185 A10W, is realized in order to fill the hole and produce the core part of the preform. Figure 2 shows an example of a preform with a 3 mm central hole and a similar preform after its subsequent core filling.

Optical Materials EXPRESS

Fig. 2. Preforms: Top, 1185A TPU preform with a 3 mm central hole, bottom, central hole filled with 1185A 10W TPU.

The optical fiber is then drawn using a home-made drawing tower using an inductive heating system with an open graphite crucible. Due to the regulation process of the heating system, the heating temperature was fluctuating over 15°C with a lower crucible temperature of 310°C. This fluctuation generates a fiber diameter variation that can range from ~80 µm to ~250 µm. That results in some lengths, ~2-3 m, of fibers with smaller diameters, and other shorter lengths, ~0.5–1 m, of greater diameters. However, these length instabilities were not bringing major issues as we intend to use fibers for short links (e.g. < 0.5 m).

Using these processes, we have manufactured three types of step-index optical fibers with the dimensions listed in Table 2. For each fiber we have determined its V number, at three different wavelengths: 633 nm, 830 nm and 1300 nm by considering the smallest diameter achieved, and the corresponding estimate of number of modes using equation $M = 4{\cdot}(V^2/\pi^2)$ [22] and an $NA = 0.38$. We made the assumption that both materials have a similar dispersion characteristic that induces a negligible NA change with wavelength. We can see that the F3 fiber is approaching a few-modes fiber behaviour for wavelengths > 800 nm.

Table 2. Optical fibers produced

Fiber type	Minimal core diameter [µm]	Cladding diameter [µm]	V number at λ [nm]			Estimated number of modes at λ [nm]		
			633	830	1300	633	830	1300
F1	44	199	83.66	63.81	40.73	2'837	1'650	672
F2	10	114	19.01	14.50	9.26	147	85	35
F3	5.4	85	10.27	7.83	4.99	43	25	10

2.2. Fiber characteristics

The produced fibers have first been visually evaluated under microscope and by launching white light in them for pieces of 40 cm in length. In Fig. 3 we can see the dark fiber end face of the three fibers types and these last when guiding white light. Afterwards, the fibers attenuation was measured on 5 different F2 fibers and in 3 F1 fibers using the cut-back technique from 40 cm down to 20 cm with a sampling length of 2 cm. Attenuation values obtained for F1 and F2 fibers are listed in Table 3 with a standard deviation of +/- 0.05 dB/cm for the F2 fiber but higher (0.12, 0.19 and 0.05 dB/cm at 633, 830 and 1300 nm respectively) for the F1 fiber. To the best of our knowledge, the closest literature we can use to compare our obtained results is found in [23]. They have measured transmission losses for TPU polymer films and have obtained attenuations

Optical Materials EXPRESS

of 0.09 dB/cm (1100 nm), 0.244 dB/cm (1310 nm) and 0.288 dB/cm (1550 nm). In our case, the attenuation seems to be stable in the 600–850 nm range, but for 1300 nm, attenuation is observed to be greater and at 1550 nm, attenuation was too large to be measured with our setup. We do not have an exact explanation about our loss origins, but we can assert some comments about it. In [23], they have performed the attenuation measurements on TPU films and not waveguides, avoiding some possible waveguide induced losses. They have processed their own TPUs and, most probably, they differ from the BASF TPUs we have used here. In our case, during the production of our fibers, we have occasionally observed a rough core-cladding interface if the drawing temperature was not high enough (i.e. the 10°K above normal temperature for the 1185A alone). It is still possible that the interface is not yet smooth enough to decrease significantly our waveguide loss. Though, the losses between F1 and F2 are relatively similar indicating that the waveguide loss should be similar between those fibers. Nevertheless, absorption is an important source that may account for our losses and the main origin arises in polymers from overtone absorption of different molecular bonds [24].

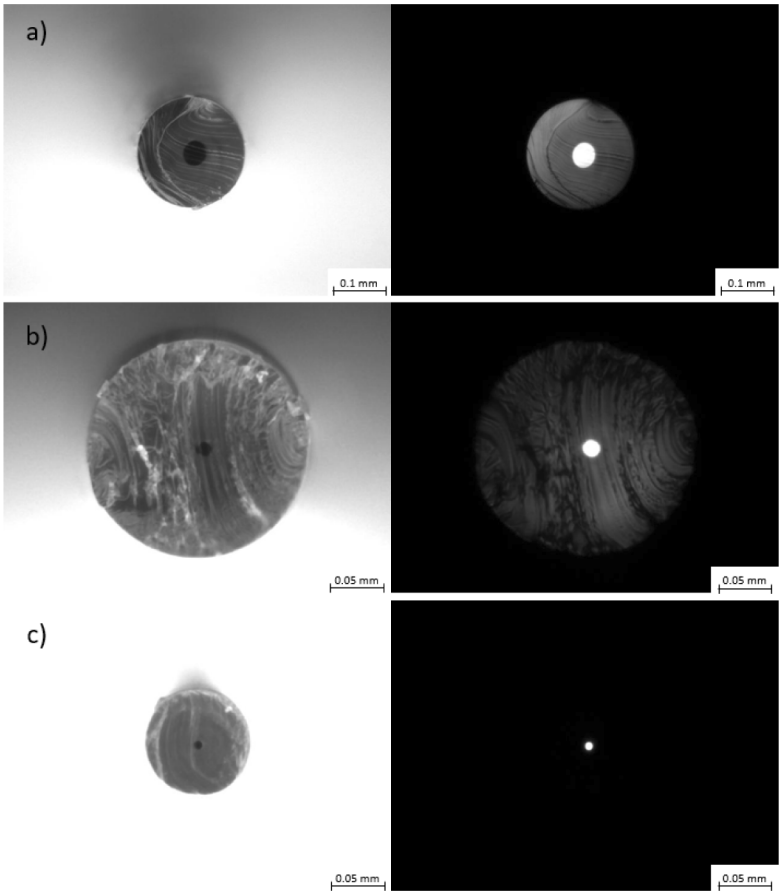

Fig. 3. Fibers produced: F1 (line a)), F2 (line b)) and F3 (line c)). Left-hand side: Illuminated endface; righ-hand side: Dark endface transmitting white light.

A second set of fiber F3 was used to measure the bending loss and results are shown on Fig. 4. Fiber was bent on metallic rods with two turns and manually maintained while the power signal was stabilizing. Results in Fig. 4 show the loss measured at a specific bending radius and referred for a 1-cm fiber length at a specific wavelength. The bending measurement was difficult because

Optical Materials EXPRESS

Table 3. Optical attenuation of F1 and F2 fibers produced

Fiber name	Attenuation at 633 nm [dB/cm]	Attenuation at 830 nm [dB/cm]	Attenuation at 1300 nm [dB/cm]
F1	0.23	0.24	0.75
F2	0.2	0.17	0.73

the TPU fibers are particularly soft. Effectively, any touch on the TPU fibers makes a direct stress on the core-cladding interface and thus a variation in the optical transmission when fiber is bent. Additionally, to bend the fiber around a rod, there is inevitably a non-negligible elongation of the fiber which induces an additional loss. Due to these uncertainties, we have added error bars in the plots and their values are +/- 0.06, 0.07 and 0.1 dB for 1300, 830 and 633 nm respectively. We can observe that losses are small enough to allow the use of the fiber in short lengths applications where small bend radius are needed.

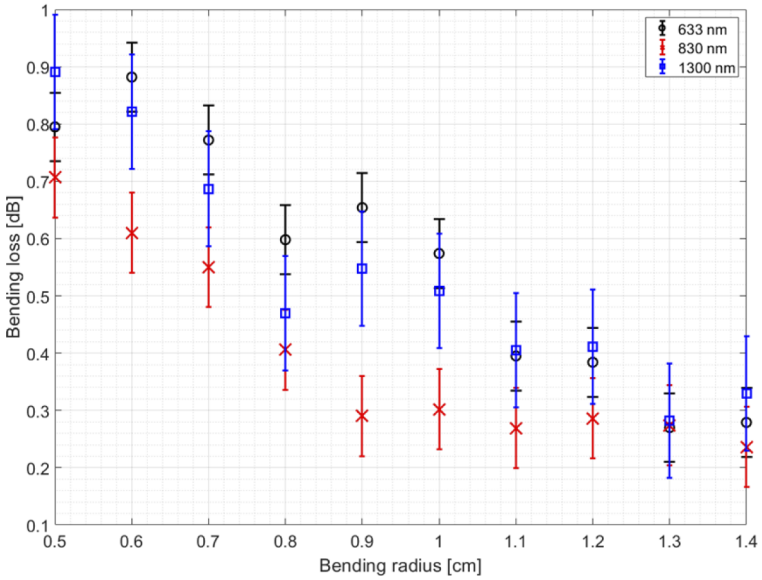

Fig. 4. Bending loss measurement for an F3 fiber at 633, 830 and 1300 nm. The loss is for a 1-cm length bent fiber.

3. Exploration of potential applications

Among the significant features that elastomeric materials bring compared to glass materials is the softness and elasticity. Softness could be very interesting in medical applications or for any reason where delicate elements need to be protected against a possible fiber scratch or break. Elasticity has a much less clear overview of its potential. So, in order to evaluate the usefulness of a true elastic optical fiber we have taken two different methods to test it. First of all, the elongation at break given for the used TPUs are of ~ 600% so we have decided to observe the far field pattern, under elongation, at the output of an F2 fiber type. A second method has been to simulate the sensing of a breath by attaching the fiber to a controlled air-filled balloon.

The elongation test used a bench where a portion of 7.8 cm, of a total 23 cm length F2 fiber, was glued in holders at its both ends as it can be seen in Fig. 5. One of the holders was fixed to the bench and the other one mobile along the fiber axis. Together with the mobile holder, a CCD camera was aligned to the fiber output in order to retrieve the far field patterns during

Optical Materials EXPRESS

the elongation. The length of the unstressed fiber between the elongated region and the CCD camera was about 2 mm leaving low probability of significant mode mixing. We launched a 633 nm laser light at the fiber input as it would generate the greater number of modes and hence a good overview of the stretching effect. Also, the use of 633 nm wavelength ensured a low loss transmission as we were expecting to elongate the fiber up to 300% leaving most probably not enough light for a camera to work at 1300 nm. Fiber was elongated by a 1 cm step and the far field pattern was recorded at each step. The resulting patterns are shown on Fig. 6 on a colored and grey scale (0 to 255 for the min and max level respectively). The real size of images is 5702.4 µm x 4276.8 µm and the distance between fiber output and the CCD sensor of about 4.3 mm. The maximum elongation achieved has been of ~128%. This maximum elongation does not correspond to a fiber break but to the gluing failure. As the gluing may not generate microbends on the fiber to avoid any distortion in the measured intensity profiles, it could not manage the slipping induced by the elongation forces. The realized elongation as allowed to decrease the core diameter to more than 30% to something around 6.6 µm from the original 10 µm. That should have decreased the mode numbers from 147 down to 64.

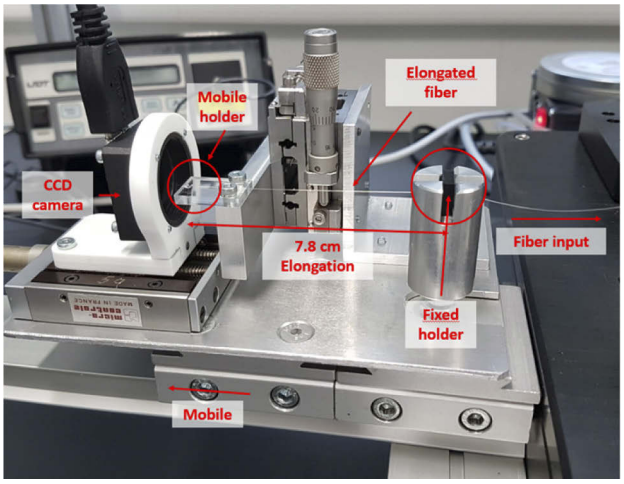

Fig. 5. Elongation setup. The red circles indicate the fiber holders: Left is on the mobile side, right is on the fixed side. 7.8 cm fiber portion is in between.

In order to get some information from these far field patterns, we have performed the $1/e^2$ diameter measurement. To do so, we have taken for each image shown on Fig. 6 the maximum intensity and have divided it by e^2. The result has allowed us to produce a binary image, as shown in Fig. 7(a) (128.2% image), where the black area is what is below the $1/e^2$ threshold and what is above it is in white. Then, by keeping all the points that are close to the binary interface we have been able to fit a circumscribed circle, as shown in Fig. 7(b), that should represent the $1/e^2$ diameter of the obtained patterns. We have measured this diameter for each elongation step and results are shown in Fig. 8. In order to consider the influence of the speckle distribution in this measurement diameter, we have added error bars on the measurement points to highlight this uncertainty, which is roughly 100 µm. We can observe a decrease tendency of the diameter when the fiber is elongated. That decrease can have two origins: a reduction of the NA and/or a decrease in the mode volume. For the first case, a reduction of the NA would be induced by a photoelastic effect on the refractive indexes. However, we believe that the change is too large to mainly originate from that effect. For the second case, a decrease on the mode volume can be brought by stripping out the higher order modes. The elongation does that stripping by decreasing the core's diameter. The remaining unstretched fiber before the output is only ~2 mm

Optical Materials EXPRESS

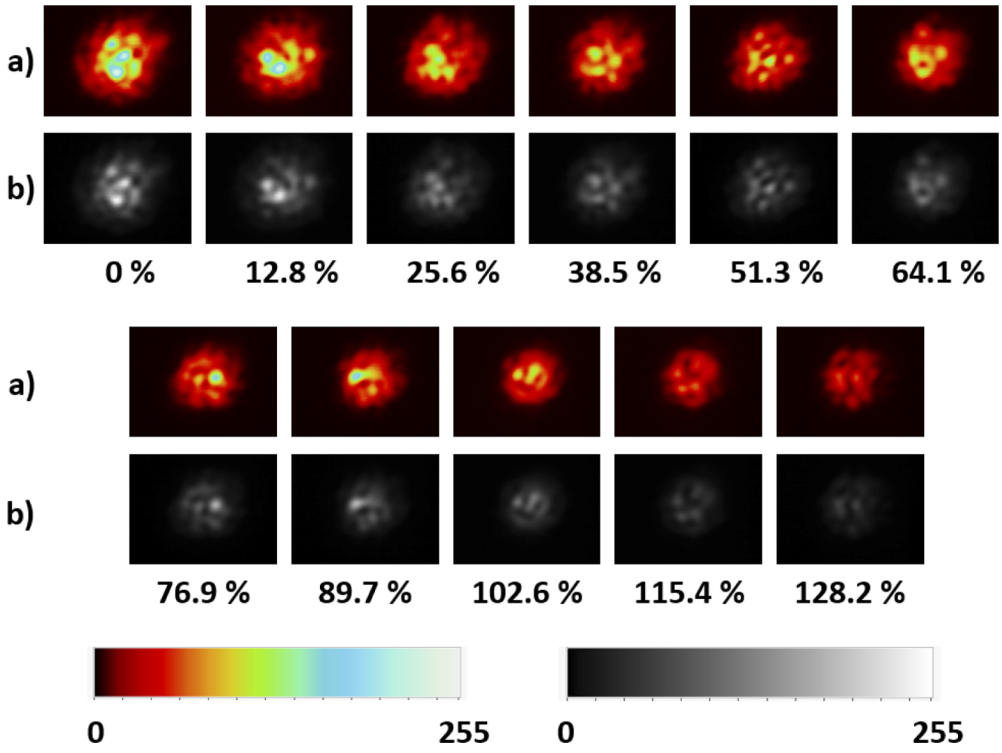

Fig. 6. Far field patterns of an F2 fiber elongated from 0 to 128.2%: a) colored scale (0 to 255); b) grey scale (0 to 255).

and shouldn't allow a mode redistribution before light exits the fiber. That makes a more reliable explanation of the observed patterns diameter decrease.

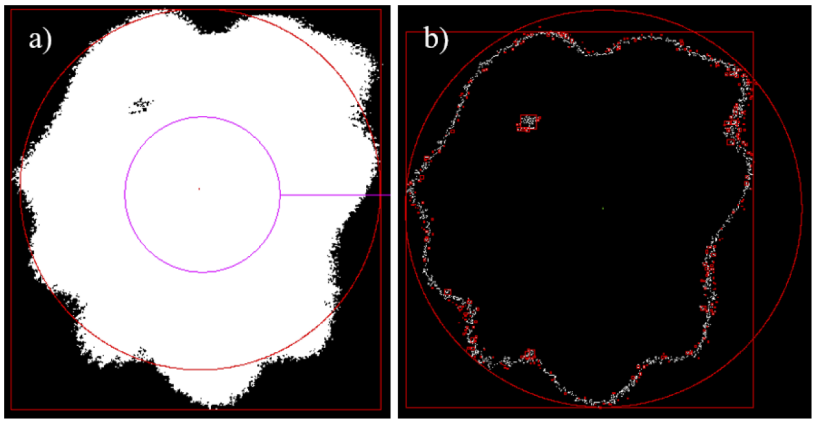

Fig. 7. Process for the $1/e^2$ measurement. Binary image (from 128.2% image) obtained from a $1/e^2$ thresholding (a) and the circumscribed circle fitting on the binary interface (b).

The breath monitoring simulation has been performed using an F2 fiber type of 1 m long. A little portion of the fiber, ~5 cm, has been simply attached with two tapes on a birthday balloon as depicted on Fig. 9. A double acting pneumatic cylinder was used to control manually the air

Optical Materials EXPRESS

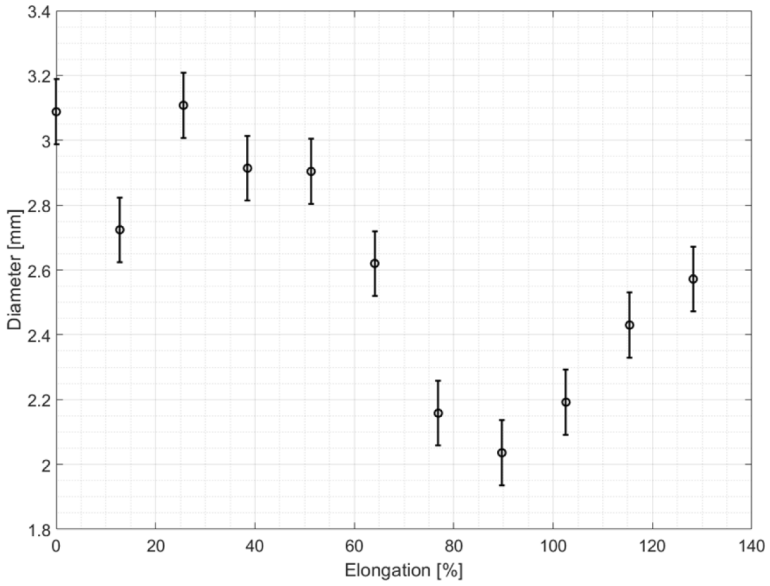

Fig. 8. Diameter retrieved from the $1/e^2$ far field patterns vs elongation induced on the fiber.

pressure inside the balloon. We have monitored the average optical transmission of a 633 nm signal sinusoidally modulated at 1 kHz through the fiber using a PDA10A-EC detector. The air pressure inside the balloon has been manually and cyclically modified and the retrieved signal can be seen on Fig. 10. The balloon was roughly inflated and deflated from a 40 mm diameter to an 80 mm diameter. The fiber experienced a change in the radius of curvature but also some stretching giving both a change in optical transmission. As shown in Fig. 10, the results clearly show that the voltage follows the geometric changes in the balloon. The signal's lack of smoothness is due to a slow sampling together with a cylinder move within the pneumatic chamber that wasn't smooth enough to avoid some little stops. Also, we can observe a slight gradual decrease in the voltage measured during the experiment. This reduction has two origins. First of all, the balloon entrance had some leaks and secondly, for each inflation, the fiber was slightly slipping from the tapes. The air leak can already be observed during the first 4 seconds where the balloon was resting. One might think that the signal should increase instead, but it decreases because the fiber curvature was increasing since the distance between tapes was

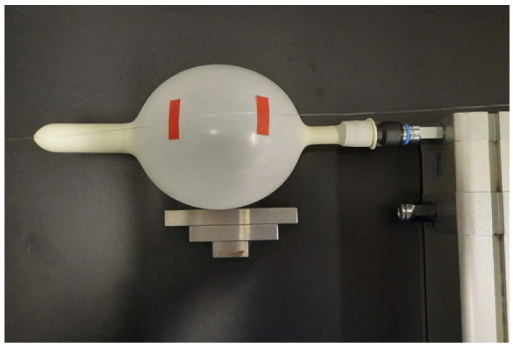

Fig. 9. Balloon test setup using a double acting pneumatic cylinder.

Optical Materials EXPRESS

decreasing. Tape slipping is inducing also a larger curvature by increasing the fiber length between the tapes. Nevertheless, we can clearly observe the monitoring of the fiber deformations on balloon's surface with a very simple and quick setup using our elastomeric optical fibers.

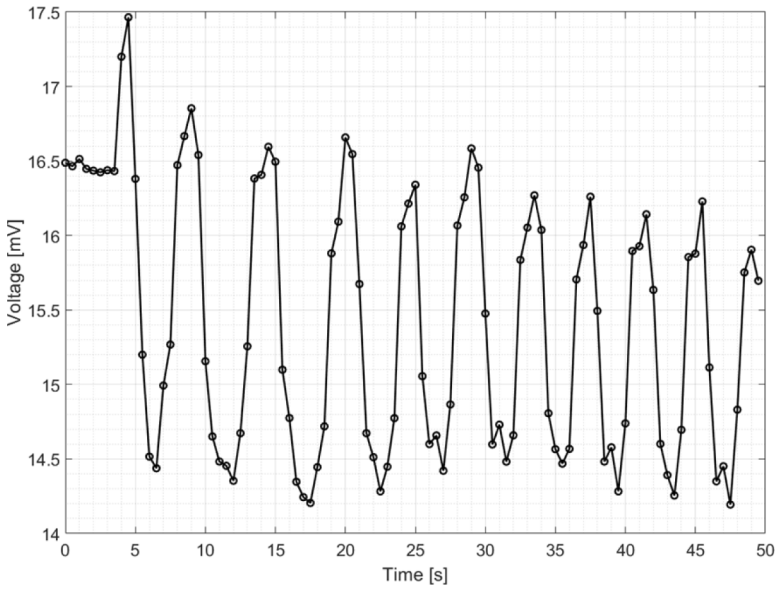

Fig. 10. Air-pressure change in a balloon sensed using an F2 type fiber.

4. Discussion

Elastomeric optical fibers present two unique features that optical fiber technology has yet to explore: Unbreakability and elasticity. Unbreakability is an unmissable parameter that drives medical applications. Traditional glass optical fibers can be found in many types and configurations today but they face a possible hazardous breakability and biocompatibility issues for long-term applications. Plastic optical fibers, as the well-known PPMA fibers, could also be good candidates but they still suffer from plastic deformations and are to be avoided in applications where complex or extreme manipulations are needed. Hence, being able to use optical fibers for a large panel of medical applications without the risk of injuries, and with materials that are already known to be used in long-term medical implantations, will have a strong impact. So, potentially, optical fiber technology could really translate its broad portfolio of fiber characteristics and configurations into applications where rigid fibers were so far limited in use.

Elasticity is a much more difficult to evaluate feature but could open a large panel of unexplored sensing behaviours and opportunities. We can start thinking about two possible opportunities of use: Micro-fibers and Fiber Bragg gratings (FBG). For micro-fibers, it is well-known that their applications range a vast panel [25,26] and polymer micro-fibers have a particular advantage. They can offer an unequalled versatility for functionalities and properties [27] and can easily be doped with functionalized dopants in order to manipulate light at the nanoscale [28]. If we can add much more elasticity to those fibers, as our fibers could do, then, better sensitivities could be achieved. For FBGs, writing a grating on our elastomeric fibers, using the point-to-point technique [29], could bring FBGs better stretchabilities. Our optical fibers could be an excellent base to produce true elastic FBGs with useful working wavelength ranges of several hundred of nm. Gratings with such stretchabilities have already been proved on volume gratings [30,31]

Optical Materials EXPRESS

and we could produce the same on our fibers by stretching them during the femtosecond laser inscription.

Regarding the used TPUs, we have used what is easily available in the market and for only one specific manufacturer: BASF. However, there is potential for having TPUs with different refractive indexes and achieve fibers with even a more reduced number of modes. For example, the BASF 1185 A10, having a refractive index n_d of 1.537, could replace our 1185 A10W and could potentially be used to produce F3 type fibers with a V number of 4.07. This would bring the realization of the first elastomeric single-mode optical fiber significantly closer.

A valuable advantage of the proposed fiber is that it can potentially be produced in industrial lengths and not just pieces of a few centimeters in length. That is a significant step ahead for real future applications. So, we can conclude that the proposed fiber will bring new opportunities for the well-being of our society and also open the door for new and unexplored sensing opportunities.

5. Conclusion

We proposed a new way to produce elastomeric optical fibers using classical injection molding of a TPU preform and then a fiber draw. We have characterized the optical behaviour of three different types of step-index optical fibers: 44, 10 and 5.4 µm core diameter fibers. Attenuations are measured to be around 0.1-0.2 dB/cm in the 633-830 nm range while they increase at 0.7-0.8 dB/cm at 1300 nm. The fibers do not guide light in the C-band optical window. The bending loss measurement has shown a high bending tolerance as the induced losses were only at ~0.8 dB/cm at a 0.5 cm bending radius. Two applications driven experiments have been performed to evaluate the potential of the produced fibers: One showing the optical behaviour of the fiber under a 128.2% elongation by observing the far field pattern, and the second one to sense a cyclic swelling and deflation of a balloon. This opens the door to unprecedented applications where traditional glass optical fibers or even plastic optical fibers show a limited flexibility and elasticity. To the best of our knowledge, this is the first elastomeric optical fibers to be produced to a few-modes configuration. The fabrication process proposed has the potential to be easily industrialized and having single-mode elastomeric optical fibers, at industrial lengths, is no longer utopic.

Funding. Innosuisse - Schweizerische Agentur für Innovationsförderung (35155.1 IP-ENG).

Acknowledgments. We would like to thank Biesterfeld Plastic Suisse AG (CH) and BASF AG (DE) for providing us the TPU granulates samples.

Disclosures. The authors declare that there are no conflicts of interest related to this article.

Data availability. Data underlying the results presented in this paper are not publicly available at this time but may be obtained from the authors upon reasonable request.

References

1. R. D. Maurer, "Glass fibers for optical communications," Proc. IEEE **61**(4), 452–462 (1973).
2. G. Keiser, F. Xiong, Y. Cui, and P. P. Shum, "Review of diverse optical fibers used in biomedical research and clinical practice," J. Biomed. Opt. **19**(8), 080902 (2014).
3. S. Nizamoglu, M. C. Gather, and S. H. Yun, "All-biomaterial laser using vitamin and biopolymers," Adv. Mater. **25**(41), 5943–5947 (2013).
4. R. Nazempour, Q. Zhang, R. Fu, and X. Sheng, "Biocompatible and implantable optical fibers and waveguides for biomedicine," Materials **11**(8), 1283 (2018).
5. S. Chen and A. Z. Weitemier, "Near-infrared deep brain stimulation via upconversion nanoparticle-mediated optogenetics," Science **359**(6376), 679–684 (2018).
6. S. Kim, T. Kyung, J. Chung, N. Kim, S. Keum, J. Lee, H. Park, H. M. Kim, S. Lee, H. Shin, and W. D. Heo, "Non-invasive optical control of endogenous Ca^{2+} channels in awake mice," Nat. Commun. **11**(1), 210 (2020).
7. R. Akhtar, M. J. Sherratt, J. K. Cruickshank, and B. Derby, "Characterizing the elastic properties of tissues," Mater. Today **14**(3), 96–105 (2011).
8. S. T. Parker, P. Domachuk, J. Amsden, J. Bressner, J. A. Lewis, D. A. Kaplan, and F. Omenetto, "Biocompatible silk printed optical waveguides," Adv. Mater. **21**(23), 2411–2415 (2009).
9. M. Choi, M. Humar, S. Kim, and S.-H. Yun, "Step-index optical fiber made of biocompatible hydrogels," Adv. Mater. **27**(27), 4081–4086 (2015).

Optical Materials EXPRESS

10. J. Guo, X. Liu, N. Jiang, A. K. Yetisen, H. Yuk, C. Yang, A. Khademhosseini, X. Zhao, and S. H. Yun, "Highly stretchable, strain sensing hydrogel optical fibers," Adv. Mater. **28**(46), 10244–10249 (2016).
11. J. Feng, Y. Zheng, S. Bhusari, M. Villiou, S. Pearson, and A. del Campo, "Printed degradable optical waveguides for guiding light into tissue," Adv. Funct. Mater. **30**(45), 2004327 (2020).
12. B. W. Swatowski, C. M. Amb, W. K. Weidner, R. S. John, and J. D. Mitchell, "Advances in manufacturing of optical silicone waveguides for high performance computing," *2014 IEEE Avionics, Fiber-Optics and Photonics Technology Conference (AVFOP)*, ThB1 (2014).
13. Md R. Kaysir, A. Stefani, R. Lwin, and S. Fleming, "Flexible optical fiber sensor based on polyurethane," *2017 Conference on Lasers and Electro-Optics Pacific Rim (CLEO-PR)*, Singapore, pp. 1–2 (2017).
14. T. Stöver and T. Lenarz, "Biomaterials in cochlear implants," *GMS Current Topics in Otorhinolaryngology - Head and Neck Surgery*, Vol. 8, ISSN 1865-1011 (2009).
15. S. Wendels and L. Averous, "Biobased polyurethanes for biomedical applications," Bioact. Mater. **6**(4), 1083–1106 (2021).
16. H. L. Narcisco Jr., "Silicone optical waveguide," US5237638A, 1991.
17. A. Stefani, S. C. Fleming, and B. T. Kuhlmey, "Terahertz orbital angular momentum modes with flexible twisted hollow core antiresonant fiber," APL Photonics **3**(5), 051708 (2018).
18. W. Belardi, "Design and properties of hollow antiresonant fibers for the visible and near infrared spectral range," J. Lightwave Technol. **33**(21), 4497–4503 (2015).
19. M. Han and A. Wang, "Exact analysis of low-finesse multimode fiber extrinsic Fabry–Perot interferometers," Appl. Opt. **43**(24), 4659–4666 (2004).
20. S. E. Golowich, W. White, W. A. Reed, and E. Knudsen, "Quantitative estimates of mode coupling and differential modal attenuation in perfluorinated graded-index plastic optical fiber," J. Lightwave Technol. **21**(1), 111–121 (2003).
21. J. G. Drobny, *Handbook of Thermoplastic Elastomers* (William Andrew Pub, 2007).
22. B. E. A. Saleh and M. C. Teich,"Fiber optics," *Fundamentals of Photonics* (Wiley, 1991), p. 283.
23. J. Jang and J. Do, "Synthesis and evaluation of thermoplastic polyurethanes as thermo-optic waveguide materials," Polym. J. **46**(6), 349–354 (2014).
24. W. Groh, "Overtone absorption in macromolecules for polymer optical fibers," Makromol. Chem. **189**(12), 2861–2874 (1988).
25. L. Tong, F. Zi, X. Guo, and J. Lou, "Optical microfibers and nanofibers: a tutorial," Opt. Commun. **285**(23), 4641–4647 (2012).
26. J-H Chen, D-R Li, and F. Xu, "Optical Microfiber sensors: sensing mechanisms, and recent advances," J. Lightwave Technol. **37**(11), 2577–2589 (2019).
27. L. Persano, A. Camposeo, and D. Pisignano, "Active polymer nanofibers for photonics, electronics, energy generation and micromechanics," Prog. Polym. Sci. **43**, 48–95 (2015).
28. P. Wang, Y. Wang, and L. Tong, "Functionalized polymer nanofibers: a versatile platform for manipulating light at the nanoscale," Light: Sci. Appl. **2**(10), e102 (2013).
29. A. Martinez, M. Dubov, I. Khrushchev, and I. Bennion, "Direct writing of fibre Bragg gratings by femtosecond laser," Electron. Lett. **40**(19), 1170 (2004).
30. A. Ryabchun, M. Wegener, Y. Gritsai, and O. Sakhno, "Novel effective approach for the fabrication of PDMS based elastic volume gratings," Adv. Opt. Mater. **4**(1), 169–176 (2016).
31. N. Cheng, Y. Tham, P. K. Sahoo, Y-J Kim, and V. M. Murukeshan, "Ultrafast volume holography for stretchable photonic structures," Opt. Express **27**(9), 12196–12212 (2019).